

Prediction of mild steel weld properties using artificial neural network and regression analysis

¹Joseph I. Achebo and ²Martins Ufuoma Eki

¹Department of Production Engineering University of Benin, Benin City, Nigeria

²Department of Mechanical Engineering Federal University of Petroleum Resources
Effurun, Delta State, Nigeria

E-mail: ¹josephachebo@yahoo.co.uk; ²eki.martins@fupre.edu.ng

Abstract

Safety hazards resulting from structural material failure occur mostly in less developed countries where material standard specifications are not strictly adhered to, due to failure of government policy implementation. These hazards often result in loss of life. Failures tend to occur at welded joints, and various research institutions are making attempts to prevent such failures by developing new methods that could predict and improve welded joint qualities. The concern goes beyond safety, but also encompasses economic and other similar long term considerations. In this study, experimental methods were used to obtain the Bead Height (BH), Ultimate Tensile Strength (UTS) and Brinell Hardness Number (BHN) of mild steel welded joints. Thereafter, the artificial neural network (ANN), and Regression analysis methods were applied to predict the corresponding values of the BH, UTS, and BHN. The resulting performance of these two predictive methods was compared side by side to determine which one of the two methods better predicted these quality properties. This comparative analysis was carried out by comparing the percentage error of ANN to that of the Regression analysis. From the results obtained, it was found that for the bead height, Regression analysis method produced a total of 1.72% error. For UTS, ANN method produced a total of 63.31% error whereas Regression analysis produced a total of 0.39% and for BHN, ANN method produced a total of 353.86% error whereas, Regression analysis method produced a total of 2.58% error. The results shows that overall, regression analysis method predicted the properties better. Also, the effect of the process parameters on the weld properties were investigated. In this study, a step by step method is applied.

Keywords: Bead height, Ultimate tensile strength, Brinell hardness number, welding process parameters, Regression analysis, Artificial neural network.

1. Introduction

Weak structural materials are a major problem in both the manufacturing and service industries. When these structural materials are under-designed to carry heavy loads, the entire structural material collapses. For major structural projects, loss of life could occur. Both human and financial resources expended are lost and ensuing litigation may attract huge sums in settlements. These accidents are not uncommon in Nigeria, but they usually go unreported, except for the exceptional incidents. In order to prevent the recurrence of these failures, it has become imperative that the root cause of these problems should

be investigated and solved. The major root cause of the problem was found to be the low strength nature of welded joints. For the fact these welded joints are lower in strength than their parent metal, it is obvious that they may not be able to withstand the same level of load (in the case of very heavy load) as the load ordinarily sustained by the parent metal.

One major way of solving this problem, is to pre-determined the strength and quality factors of the weld, before welding in such a way that the manufacturer knows in advance the quality of joint he/she is about to produce that would fit a particular load, it is intended to carry. This

preemptive effort could help to save time, and conserve financial, material, and human resources.

In current research, several models have been adopted for predicting the strength and quality factors of welded joints. These models were developed, after years of intensive research, to simplify the forecasting process of the properties of any material. In this study, the ANN and regression analysis models were applied.

A weld's mechanical properties determine the actual status of the weld joint. There are myriads of combinations and proportions of constituent elements, and techniques for welding, tailored to various specifications. This is the reason research into obtaining better and a reliable weld property is unending.

It is imperative that a weld joint of high quality should be produced on the first try of the welding operation because attempting several welding operations, just to produce a weld of high quality can be costly and therefore uneconomical. Therefore, in order to save time and attain precision and accurate prediction, mathematical models are applied. These models provide figures that reveal predetermined responses and aid in obtaining near optimal mechanical properties. The deviation from the mean of responses obtained is usually very minute.

Researchers globally have applied both artificial neural network (ANN) and regression analysis (RA) in predicting weld bead geometry and its mechanical properties. These include, the works of Campbell et al. (2012), who predicted weld geometry made by the gas metal arc welding process, in addition to alternating shielding gases by applying the artificial neural network. The authors compared the experimental and predicted results, which show that ANN can successfully generate a model that can predict multiple weld

geometries when compared with experimental results. Achebo (2015), developed a predictive model for determining mechanical properties of AA6061 using regression analysis it was found that the predicted mechanical properties using regression analysis compared well with those obtained by experimental procedure. Sen et al. (2014), used the regression analysis method to predict weld bead geometry using double gas metal arc welding process and the confirmation experimental test results show that the regression model predicted the bead geometry with reasonable accuracy.

2. Materials and methods

2.1 Materials

The Gas Metal Arc Welding (GMAW) machine was used to weld 4 mm mild steel plates. The input parameters used for this study are current, voltage, welding speed and welding angle. The GMAW welding machine contains the welding gun, shielding gas consisting of 80% argon and 20% carbon dioxide. A 3.2 mm consumable wire electrode of AWS classification ER70S-3 was used for the welding operation.

2.2 Methods

2.2.1 Brinell Hardness Test

The Brinell hardness tester was used in this study to determine the weld or test specimen's hardness number. The higher the Brinell hardness number (BHN), the harder the specimen becomes.

2.2.2 Tensile Test

The other equipment used is the Avery Universal tensile testing machine. This tensile tester has a computer monitor attached to it. As the tensile tester pulls the tensile specimen apart to a breaking point, the properties such as the ultimate tensile strength, yield strength, percentage elongation, and percentage reduction in area

etc, are displayed on the screen of the computer monitor.

2.2.3 Bead height measurement

The sixteen process parameters were used to make weldments. Each combination of process parameters were used to make five weldments and each of these weldments were bisected. The bead height (BH), of each of the five weldments were measured using a caliper micrometer and the average value of the bead heights was recorded. Eighty weldments were made with the sixteen process parameters and sixteen average values of the bead heights were recorded.

2.2.4 Power saw

Power saw was used to cut the weld bead so that the bead height can be measured. The sawing machine is a machine tool designed to cut material to a designed length or contour. It functions by drawing a blade containing teeth through the work piece. The

sawing machine is preferred to the hand saw since it is faster and easier and principally produces an accurate square or mitered cut on the work piece. The power hacksaw is used for squared or angle cutting of metal. It uses a reciprocating (back and forth) cutting action.

2.2.5: Artificial neural network

A feed-forward back-propagation neural network with two (2) layers, four (4) inputs, two (2) outputs and ten (10) neurons was used to simulate the system. Seventy percent (70%) of the input vectors was used to train the network, fifteen percent (15%) to validate and the remaining fifteen percent (15%) to test the network.

The neural network model uses a Laveberg-Marquardt training function, a learn_gdm adaptive learning function, a mean squared error (mse) performance function, a log-sigmoid transfer function for layer 1 and a linear transfer function for layer 2 (see Fig 1).

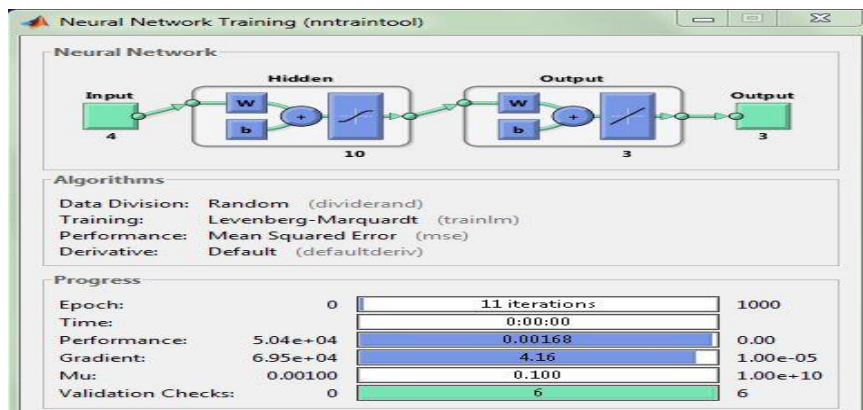


Fig.1 Neural Network diagram

Input and target data as shown in Table 1 was fed to the network. The network trains itself and learns the pattern or relationship between the inputs and targets. It then predicts output

based on the learned pattern and minimizing the error (i.e. the difference between the targets and the outputs) in the process.

2.2.6: Procedure

The following steps were utilized in predicting and optimizing the welding process parameters:

1. The GMAW machine was used to make weld deposits for each welding operation
2. The weld deposits were machined into the tensile specimen which were used to conduct tensile test. From the used

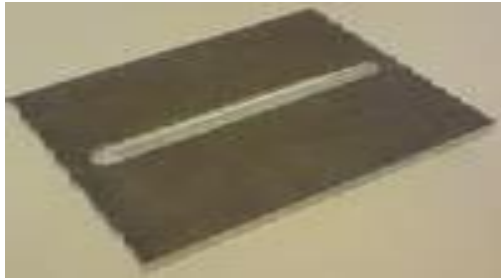


Fig 2 Test specimen

tensile specimen the hardness numbers were determined. Weldments were also bisected to measure the bead height (see Fig. 2).

3. The artificial network model was applied
4. A multiple linear regression model was subsequently applied.
5. The results from 3 and 4 above were compared to determine which best fit the experimental data.

3 Results and discussion

3.1 Presentation of results

3.1.1 Application of neural network

The sixteen inputs and targets vectors were randomly divided into three groups. 70% of the vectors were used to train the network, 15% used to validate and the remaining 15%

to test the network. The results are as shown in Figs 3, 4 and 5. The overall performance shows a mean squared error of 4.3996 with eight (8) iterations in two seconds. From the regression plot, the R values for training, validation and test are respectively: 0.989885, 0.66052 and 0.71901. The overall R value is 0.89082.

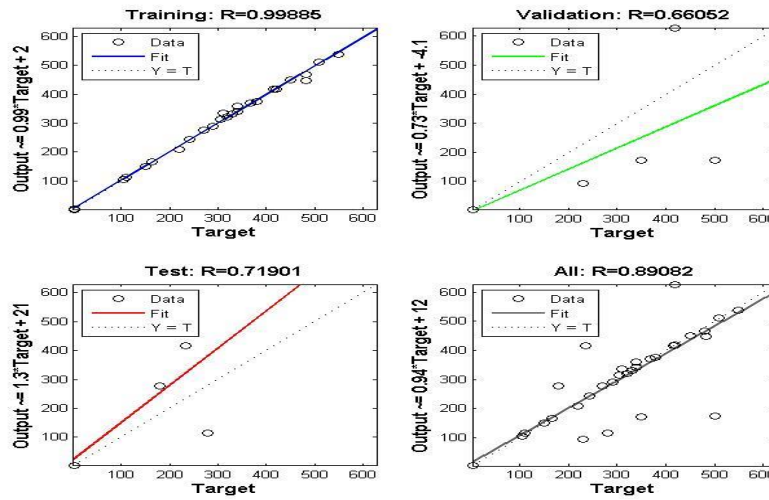


Fig 3 Regression Plots of Neural Network Analysis

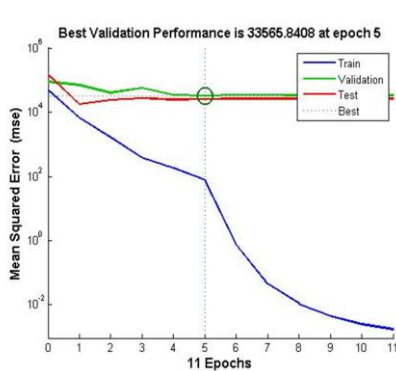


Fig 4 Performance Plot

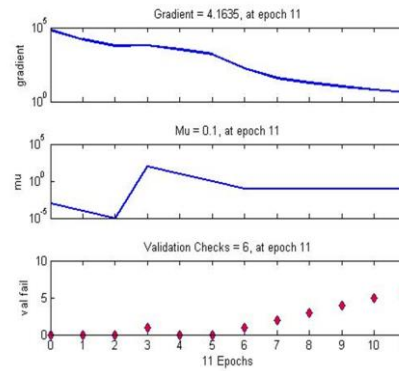


Fig 5 Training State

3.1.2 Regression Model

A first degree linear model of the form $Y_i = \beta_0 + \beta_1 I + \beta_2 V + \beta_3 S + \beta_4 f + \epsilon_i$ is proposed for the system. Where β_0 , β_1 , β_2 , β_3 , β_4 and ϵ_i are the intercept, predictor parameters and error term respectively.

In this study, the predictive model equation developed by using the regression analysis for predicting the BHN, UTS and BH are as follows:

$$BHN = 512.337 + 0.024*I - 7.230*V - 1.144*S + 0.554*A \quad (1)$$

$$UTS = 540.024 - 0.291*I + 0.353*V - 0.529*S + 0.266*A \quad (2)$$

$$BH = 1.11 - 0.003*I + 0.013*V - 0.024*S - 0.007*A \quad (3)$$

3.1.3 Comparing ANN Model and Regression Model

Tables 1-3 show the comparison between the experimental and predicted response variables using ANN and Regression models.

Table 1: Bead height results compared

| Current (A) | 30 | 1.80 | Welding Angle, A (°) | Bead Height (Experimental) | Predicted Bead Height (ANN) | Predicted Bead Height (Regression) |
|-------------|----|------|----------------------|----------------------------|-----------------------------|------------------------------------|
| 420 | 30 | 2.10 | | | 2.632 | 2.096 |
| 420 | 30 | 3.20 | | | 2.034 | 2.229 |
| 420 | 28 | 135 | | | 2.491 | 3.053 |
| 420 | 28 | 135 | 90 | 2.65 | 2.687 | 2.629 |
| 310 | 28 | 135 | 90 | 3.44 | 2.560 | 2.994 |
| 420 | 18 | 135 | 90 | 1.95 | 1.985 | 2.496 |
| 310 | 20 | 100 | 90 | 2.05 | 2.191 | 2.064 |
| 420 | 18 | 135 | 30 | 3.46 | 3.190 | 2.920 |
| 420 | 28 | 100 | 90 | 1.92 | 1.850 | 1.805 |
| 420 | 28 | 135 | 30 | 2.33 | 2.491 | 3.053 |
| 310 | 18 | 135 | 90 | 2.61 | 3.227 | 2.861 |
| 310 | 18 | 110 | 90 | 2.38 | 2.385 | 2.273 |
| 420 | 28 | 100 | 30 | 3.10 | 2.034 | 2.229 |
| 310 | 18 | 135 | 30 | 3.62 | 3.124 | 3.285 |
| 310 | 18 | 100 | 90 | 2.16 | 2.182 | 2.038 |
| 310 | 28 | 100 | 30 | 1.85 | 2.442 | 2.595 |

Table 2 UTS results compared

| Current (A) | Voltage (V) | Speed (S), mm/s | Welding Angle, A (°) | UTS (Experimental) | Predicted UTS (ANN) | Predicted UTS (Regression) |
|-------------|-------------|-----------------|----------------------|--------------------|---------------------|----------------------------|
| 420 | 18 | 100 | 30 | 420 | 627.823 | 379.179 |
| 420 | 28 | 100 | 30 | 415 | 417.109 | 382.707 |
| 420 | 28 | 135 | 30 | 250 | 538.227 | 364.181 |
| 420 | 28 | 135 | 90 | 320 | 320.372 | 380.131 |
| 310 | 28 | 135 | 90 | 500 | 172.515 | 412.146 |
| 420 | 18 | 135 | 90 | 450 | 449.865 | 376.604 |
| 310 | 20 | 100 | 90 | 380 | 376.358 | 427.849 |
| 420 | 18 | 135 | 30 | 420 | 418.893 | 360.654 |
| 420 | 28 | 100 | 90 | 330 | 331.194 | 398.656 |
| 420 | 28 | 135 | 30 | 550 | 538.227 | 364.181 |
| 310 | 18 | 135 | 90 | 310 | 335.923 | 408.619 |
| 310 | 18 | 110 | 90 | 482 | 448.292 | 421.851 |
| 420 | 28 | 100 | 30 | 234 | 417.109 | 382.707 |
| 310 | 18 | 135 | 30 | 242 | 243.939 | 392.669 |
| 310 | 18 | 100 | 90 | 481 | 467.752 | 427.144 |
| 310 | 28 | 100 | 30 | 510 | 511.413 | 414.722 |

Table 3: BHN Predictive Results using ANN and Regression Analysis

| Current (A) | Voltage (V) | Speed (S), mm/s | Welding Angle, A (⁰) | BHN Experimental | Predicted BHN ANN | Predicted BHN Regression |
|-------------|-------------|-----------------|-----------------------------------|------------------|-------------------|--------------------------|
| 420 | 18 | 100 | 30 | 350 | 170.970 | 294.363 |
| 420 | 28 | 100 | 30 | 110 | 113.858 | 222.063 |
| 420 | 28 | 135 | 30 | 180 | 276.207 | 182.012 |
| 420 | 28 | 135 | 90 | 150 | 149.846 | 215.275 |
| 310 | 28 | 135 | 90 | 230 | 92.504 | 212.675 |
| 420 | 18 | 135 | 90 | 340 | 340.476 | 287.575 |
| 310 | 20 | 100 | 90 | 290 | 289.546 | 310.566 |
| 420 | 18 | 135 | 30 | 105 | 104.954 | 254.312 |
| 420 | 28 | 100 | 90 | 330 | 331.779 | 255.326 |
| 420 | 28 | 135 | 30 | 270 | 276.207 | 182.012 |
| 310 | 18 | 135 | 90 | 220 | 209.066 | 284.975 |
| 310 | 18 | 110 | 90 | 340 | 359.564 | 313.583 |
| 420 | 28 | 100 | 30 | 280 | 113.858 | 222.063 |
| 310 | 18 | 135 | 30 | 368 | 370.548 | 251.712 |
| 310 | 18 | 100 | 90 | 305 | 314.239 | 325.026 |
| 310 | 28 | 100 | 30 | 165 | 166.221 | 219.463 |

Table 4: Percentage Error of Weld Properties

| Bead height, mm | | UTS, (MPa) | | BHN | |
|------------------------|------------------------|------------------------|------------------------|------------------------|------------------------|
| % error _{ANN} | % error _{Reg} | % error _{ANN} | % error _{Reg} | % error _{ANN} | % error _{Reg} |
| -31.6109 | -14.1221 | -33.1022 | 10.7656 | 104.7143 | 18.9008 |
| 3.2448 | -5.7874 | -0.5056 | 8.4381 | -3.3884 | -50.4645 |
| 28.4625 | 4.8149 | -53.5512 | -31.3528 | -34.8315 | -1.1054 |
| -1.3770 | 0.7988 | -0.1161 | -15.8185 | 0.1028 | -30.3217 |
| 34.3750 | 14.8965 | 189.8299 | 21.3162 | 148.6379 | 8.1462 |
| -1.7632 | -21.8750 | 0.0300 | 19.4889 | -0.1398 | 18.2300 |
| -6.4354 | -0.6783 | 0.9677 | -11.1836 | 0.1568 | -6.6221 |
| 8.4640 | 18.4932 | 0.2643 | 16.4551 | 0.0438 | -58.7121 |
| 3.7838 | 6.3712 | -0.3605 | -17.2219 | -0.5362 | 29.2465 |
| -6.4633 | -23.6816 | 2.1874 | 51.0238 | -2.2472 | 48.3419 |
| -19.1199 | -8.7732 | -7.7170 | -24.1347 | 5.2299 | -22.8002 |
| -0.2096 | 4.7074 | 7.5192 | 14.2584 | -5.4410 | 8.4242 |
| 52.4090 | 39.0758 | -43.8996 | -38.8566 | 145.9204 | 26.0903 |
| 15.8771 | 10.1979 | -0.7949 | -38.3705 | -0.6876 | 46.1988 |
| -1.0082 | 5.9863 | 2.8323 | 12.6084 | -2.9401 | -6.1614 |
| -24.2424 | -28.7091 | -0.2763 | 22.9739 | -0.7346 | -24.8165 |
| | | | | | |

| | | | | | |
|----------------|---------------|----------------|---------------|-----------------|---------------|
| 54.3863 | 1.7153 | 63.3074 | 0.3898 | 353.8595 | 2.5748 |
|----------------|---------------|----------------|---------------|-----------------|---------------|

3.1.4 Determination of Percentage Error (% Error)

Percentage error is determined as follows:

$$\% \text{ error} = \frac{\text{experimental value} - \text{predicted value}}{\text{predicted value}} \times 100 \quad (4)$$

Percentage error is a percentage in the form of relative change calculated from the absolute change between the experimental (measured) and theoretical (predicted) values and dividing by the theoretical (predicted) value. When a percentage error value is very close to zero, it means that it is very close to the targeted value, which is good.

The percentage error for the bead height, UTS and BHN using ANN and Regression analysis are tabulated in Table 4.

3.2 Discussion

Tables 1 - 3 show the comparison between the experimentally determined bead heights, UTS and BHN respectively and the predicted bead heights, UTS and BHN using ANN and regression analysis respectively.

From Tables 1- 3 it is seen that Regression analysis was a better model than ANN in predicting the bead height, UTS and BHN. From Tables 1- 3 the deviation of the predicted bead height, UTS and BHN from the experimental values appear to be more with the predicted values using ANN.

Table 4 shows the percentage error determination of both the mechanical and bead geometry properties using the artificial neural network and the regression analysis. The results in this table for the bead height, reveals

This makes it susceptible to impact loads. More so, it also becomes very hard because of its brittle nature. In this case, the molten metal has solidified but grain lattice vacancies might exist in the weld microstructure. These vacancies may likely increase the depth of indentation during the BHN mechanical test. The higher the

that using the regression analysis predicted the weldment properties to up to over 90% precision over using the artificial neural network for the bead height, UTS and BHN. This analysis confirms the interpretation given by Tables 1 - 3.

3.2.1 Effect of welding process parameters on the weld mechanical properties

Fig 6(a) shows the relationship between the welding current and the Brinell hardness number. In Fig 6(a), it is found that as the current increases, the Brinell hardness Number reduces. This indicates that very high current can deform the weldment by excessively heating and agitating the atomic structures of the weldment. This prolonged heating of the weldment in most cases allows enough time for atmospheric air to intermix with the molten weld metal thereby oxidizing these atoms, which makes the atoms transit from their microstructural state to the macrostructural state because of oxidation. In that oxidized macrostructural state, the weld metal becomes less dense with possible presence of air spores which lower the quality of the weldment. At this point, the BHN of these macrostructure weldments are usually low.

However, when the weldment becomes denser and finer, the BHN increase. The BHN is a measure of the hardness value of the weldment. Therefore, as the weldment becomes oxidized, it enhances its chances of being brittle.

indentation in the weldment, the lower the BHN.

Fig 6 (b) shows the relationship between BHN and voltage. From Fig 6(b), the increase in voltage reduce BHN of weldments. This indicates that the greater the welding voltage, the greater the flow of the welding current and the more the arc that is dissipated. However, a voltage may actually produce an electrostatic

field, which can occur when no current flows but as the voltage increases between two separate points by a specific distance, the electrostatic field becomes more intense. As these separate points widen, the electrostatic flux density present within this widened separate points reduces. Electrostatic field is an electric field associated with static or fixed electric charges. These charges consist of the positive and negative charged electrodes.

Summarily, the welding voltage initializes the arc, which in this case, melts the welding electrode and part of the parent metal. Increasing the voltage may likely widen the heat affected zones (HAZ). This shows that more volatile strength allowing elements present in the parent metal may vaporize thereby weakening the strength of the post heat treated parent metal. This process would eventually affect its hardness value.

Fig 6(c) shows the relationship between the BHN and welding speed. From Fig 6(c), as the welding speed increase, the BHN also increases. This indicates that as the welding speed increase, the welding time reduces and the microstructure of the weldment becomes finer. Finer microstructure produces a dense weldment which means increased strength, increased hardness and higher weldment quality. A dense microstructure usually has no gas entrapped spores present in the weldment. The weldment however, is expected to be ductile and of high strength.

Fig 6(d) shows the relationship between the welding angle and the BHN. As the welding angle increases, the BHN also increase. This indicates that the welding angle could to a great extent determine the arc length. The shorter the arc length the more, the

Closely packed microstructural grains are dense and possess high strength. Therefore, as the welding voltage increase, the UTS is likely to also increase.

Fig 7(c) shows the relationship between welding speed and UTS. From Fig

effect of the arc heat would be on the weldment and the spread of this arc heat also determines the size of the heat affected zones (HAZ). The size of the heat affected zone can determine the level of the quality of the weldment microstructure.

Therefore, when the positioning of the welding torch attracts a lot of arc heat to the weldment, spatter may form. This spatter which is in the molten state upon cooling could absorb moisture, and moisture absorbed by the molten weldment oxidizes it and leaves the cooled weldment in the brittle state. This state is assumed to be hard in nature. Summarily, as the welding angle increases, it would eventually increases the BHN of the weldment.

Fig 7(a) shows the relationship between the welding current and the UTS of the weldments. From Fig 7(a), it is observed that as the welding current increases, the UTS also increases. This indicates that, since the current is within the range of current expected to be high enough to form spatter. It heats the weldment and creates fine microstructure which is known to possess high strength, and weldment with high strength is expected to have high UTS.

Fig 7(b) shows the relationship between the welding voltage and the weldment UTS. From Fig 7(b), it is shown that as the voltage increases, the UTS also increases. The effect of the voltage on weldment is similar to the effect of current on weldment. In this case the voltage generate significant electrostatic flux density which produces enough arc heat to form molten weldments. The metal grains in the solidified weldment microstructure is homogeneously distributed, which makes the grains closely packed.

7(c), it is found that the higher the welding speed, the lower the UTS. This indicates that when the welding speed is high, not enough arc heat may be produced to make weldment. This dearth of arc heat is likely to produce heterogeneous microstructure of the

weldment. This microstructural view is likely to lower the weld quality, which would eventually reduce its UTS. UTS is a vital measure of weldment ductility. Very high welding speed has been found not to enhance UTS.

Fig 7(d) shows the relationship between welding angle and UTS. From Fig 7(d), it can be found that as the welding angle increases, the UTS decreases. This indicates that the positioning of the welding torch during the welding operation affects the UTS of the weldments. Therefore a lower welding angle of between 300 and 400 would produce high UTS falling between the range of 420MPa and 550MPa. In this case, a lower welding angle is recommended.

Fig 8(a) shows the relationship between the welding current and bead height. As the current increase, the bead height also increases. This indicates that the higher the current, the more arc heat is produced to melt the electrodes/filler wires and slightly part of the base metal to form a weldment. Furthermore, when the electrodes/filler wires are sufficiently melted, the molten weld metal deposits flow into the base metal to be joined together to form a fusion. The level of molten weld metal penetration into the base metal from where the bead height can be measured is obtained upon solidification. Summarily, the discussion above shows that the higher the welding current, the higher the molten weld metal deposited in between the base metals to be joined, the higher the weld bead penetration, the more the bead height obtained.

Fig 8(b) shows the relationship between the welding voltage and the bead

height. As the voltage increases, the bead height also increases. The welding voltage initiates the arc heat that causes a large bead hump. This eventually would create a large bead height. Since smaller bead heights are desirable, it would be recommended to utilize lower values of the welding voltage that are within the range of values considered in this study.

Fig 8(c) shows the relationship between the welding speed and the bead height. As the welding speed increase, the bead height reduces. It has been mentioned in this study that the higher the welding speed, the lower the welding time and the lower the heat affected zone created. This however is as a result of the welding operation which appears to be concentrated on localized area.

Localized welding forms a well guided weld bead deposition and as a result of this type of welding operation, small bead heights and widths are expected to be produced therefrom.

Fig 8(d) shows the relationship between the welding angle and the bead height. As the welding angle increases, the bead height decreases. This indicates that the positioning of the welding torch affects the buildup of the weld metal deposition. As the welding torch is moved away from the weldment during a welding operation, the effect of the arc heat on filler wire reduces. This circumstance optimizes the effect of the arc heat on the filler wire so that it does not cause spatter, instead it forms a well guided slurry flowing molten weldment into the parent/basemetal joints producing weld beads with small heights, widths and high penetration.

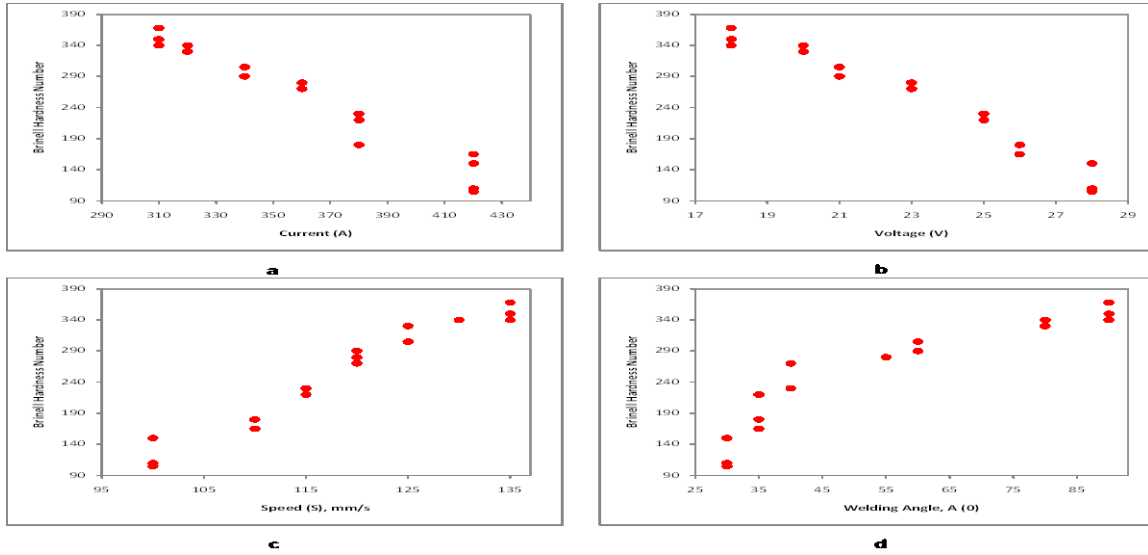


Fig 6 Plot of BHN against input parameters

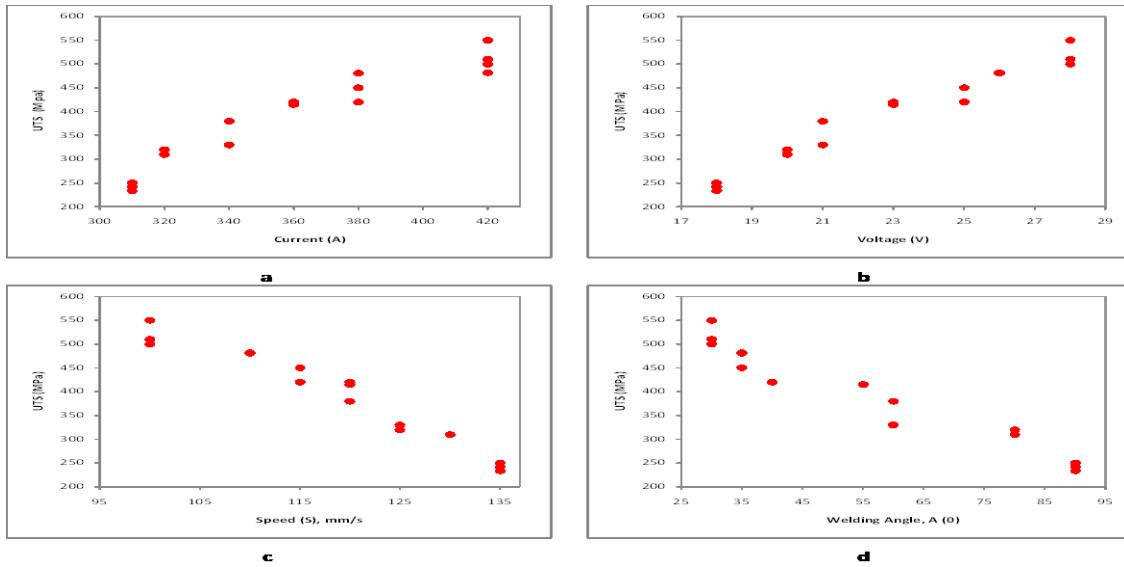


Fig 7: Ultimate tensile strength against input parameters

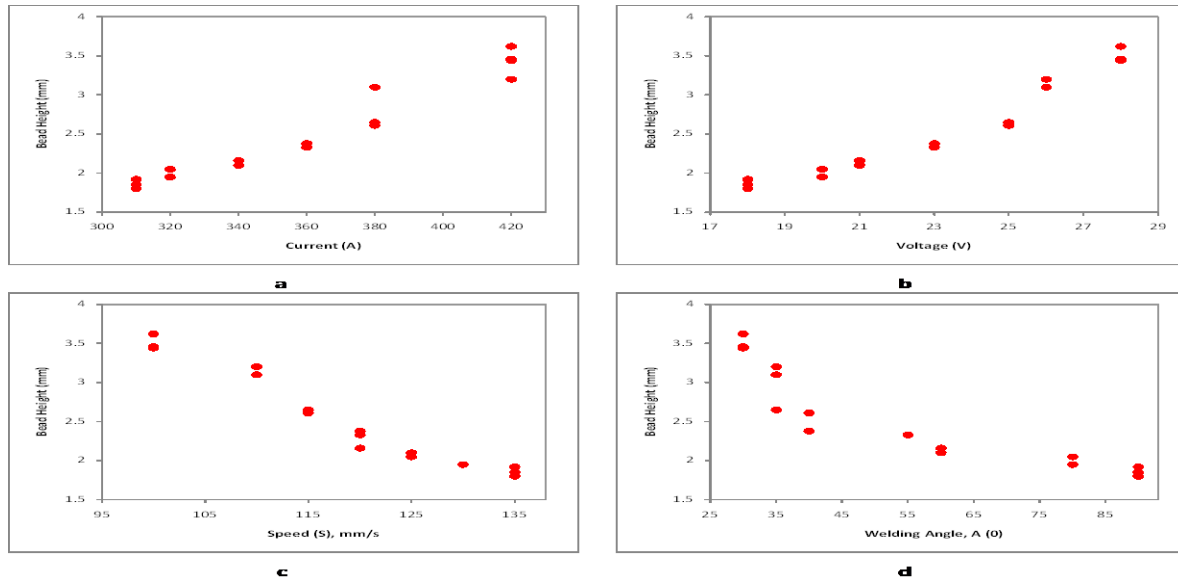


Fig 8: Bead height against input parameters

Conclusion

In this study, mild steel weld properties, such as the bead height, ultimate tensile strength and the Brinell hardness number were determined experimentally. This implies that after the welding operations using the gas metal arc welding (GMAW) process, the weld beads were bisected using a power saw and measured with a micrometer. The weldments were machined into tensile test samples and their UTS determined using the universal tensometer. These weldments were also polished and etched with sodium hydroxide solution and their BHN were determined by using the Brinell hardness tester.

In this study, the input variables are the process parameters and the output variables are the test and measured results. The ANN and regression analysis models are applied to this study for predicting the values of the bead height, UTS and BHN. This prediction is relevant for pre-determining these weld properties before the welding operation to avoid unnecessary wastage of material and human resources and also to save time. Handy predicted

values help the Project Engineer to plan and manage his/her project proposals.

From the results obtained in this study, it can be deduced that the regression analysis model was able to make a much better prediction than using the ANN model. From Tables 1-3, it can be seen that the ANN model was not able to precisely predict these mild steel weld properties, which is contrary to the claims made by Campbell et al. (2012) and Towsyfyhan et al. (2013).

The effect of the process parameters such as the current, voltage, welding speed and welding angle on the weld properties such as the bead height, UTS and BHN were investigated. This investigation was done to determine the extent to which these process parameters impacted on the output results of the weld properties.

Reference

Achebo, J., 2015. "Development of a predictive model for determining mechanical properties of AA 6061 using regression analysis" *Production & Manufacturing Research*. An Open Access Journal

Joseph I. Achebo and Martins Ufuoma Eki: Prediction of mild steel weld properties using artificial neural network and regression analysis

3(1):169-184, DOI: 10.1080/21693277.2015.1025447.

Campbell, S. W., Galloway, A. M. and Mcpherson, N. A., 2012. "Artificial Neural Network Prediction of Weld Geometry Performed Using GMAW with Alternating Shielding Gases". *Welding Journal*, 91:174s – 181s.

Sen, M., Mukherjee, M. and Pal, T. K., 2014. "Prediction of weld bead geometry for double pulse gas metal arc welding process by regression

analysis", *5th International Design and Research Conference*, IIT Guwahati, Guwahat, pp 814-6.

Towsyfy, H., Davoudi, G., Pbahram, P., Dehkordy H. and Kariminasab A., 2013. "Comparing the Regression Analysis and Artificial Neural Network in Modeling the Submerged Arc Welding (SAW) Process" *Research Journal of Applied Sciences, Engineering and Technology*. 5(9): 2701-2706.